



# STRUCTURAL, OPTICAL, MORPHOLOGICAL, AND MAGNETIC PROPERTIES OF $MgFe_2O_4$ (MF) NANOPARTICLES

Prof.G.Pakardin<sup>1\*\*</sup>, Kongi Prasad<sup>2</sup>, D.Chinna Venkata Subbaiah<sup>2</sup>, P.Ameena<sup>2</sup>, Dr. K.Evangili Supriya<sup>3</sup>, Dr. S Dastagiri<sup>3\*</sup>, Prof. MV Lakshmaiah<sup>3</sup>

<sup>1</sup>Department of Physics, SCNR Govt. Degree College, Proddatur, YSR Kadapa,, A.P., India.

<sup>2</sup>Department of Physics, Yogi Vemana University, YSR Kadapa, A.P., India.

<sup>3</sup>Department of Physics, Sri Krishnadevaraya University, Anantapuramu, A.P., India.

**Abstract:**  $MgFe_2O_4$  (MF) nanoparticles synthesized through hydrothermal method. The structural, optical, morphological, and magnetization of  $MgFe_2O_4$  nanoparticles were carried by XRD, UV-VIS, FT-IR, PL, FE-SEM with EDX, and VSM techniques, respectively. It is confirmed that the prepared sample has a cubic structure in nature through XRD. The crystallite size is determined by Debye-Scherrer formula. The Optical properties are such as UV- Visible FT-IR, and PL was estimated by an energy band gap, the formation of the ferrite have been phase confirmed and the studies reveal that the excitation wavelength is at 425 nm of  $MgFe_2O_4$  nanoparticles. The presence of peaks of respective elements (Mg, Fe, and O) in the EDX spectrum showed the formation of  $MgFe_2O_4$  nanoparticles. The magnetic properties were estimated by VSM.

**Keywords:-** XRD, Crystallite Size, FT-IR,FE-SEM, energy band gap, Hydrothermal method.

## 1. INTRODUCTION

The spinel ferrites with a common formula of  $MFe_2O_4$ , (M: Fe, Mn, Co, Ni, Cu, Zn, etc.) are a large group of this family, where  $M^{2+}$  and  $Fe^{3+}$  are the divalent and trivalent cations occupying tetrahedral (A) and octahedral (B) interstitial positions of the face centre cubic lattice formed by  $O^{2-}$  ions which have attracted attention due to their excellent magnetic and electrical properties alongside their semiconducting properties [1-3]. Beside by way of the spinel ferrites, an  $MFe_2O_4$  nanoparticle finds extensive applications in magnetic based diagnosis and treatment devices [4]. Magnesium ferrite ( $MgFe_2O_4$ ) nanoparticles as an interesting member of these materials have remarkable features such as excellent chemical stability, high coercivity, strong anisotropy, and great saturation magnetization [5]. Curie temperature is one of the important parameters for every ferrite in scintillating to its intrinsic property that could with precision control by the preferential preparation conditions, etc. The opportunity behaviors to synthesize  $MgFe_2O_4$  nanoparticles are many such as the electrospinning [6], auto-combustion method [7], co-precipitation route [8], micro-emulsion technique [9], ball milling [10], and sol-gel [11]. In addition, thermolysis [12], wet chemical co-precipitation technique [13], self-propagating and microemulsion [14, 15], are also used. In this paper, we report the structural, morphological, optical and magnetic properties of  $MgFe_2O_4$  nanoparticles by using hydrothermal method.

## 2. MATERIALS AND EXPERIMENTAL METHODS

For the synthesis of  $\text{MgFe}_2\text{O}_4$  nanoparticles, we selected the starting materials as  $\text{Mg}(\text{NO}_3)_2 \cdot 6\text{H}_2\text{O}$  (99.8% purity, Sigma-Aldrich), and  $\text{Fe}(\text{NO}_3)_3 \cdot 9\text{H}_2\text{O}$  (99.9% purity, Sigma-Aldrich). The sodium hydroxide (NaOH) pellets and its aqueous solution were also used to work as the solvent, in the hydrothermal reaction. In addition, purified water in the ratio of 1:4 (mixed precursors (gm): distilled water (ml)) is applied to the precursors and the resultant solution is placed on a magnetic stirrer. In the mean time, the NaOH aqueous solution was added drop by drop to the nitrate solution. As a result of the stirring of solution for 2 h, the white and delicious solution was obtained. This solution was further shifted to Teflon-linked bowl of 500 ml capacity and kept in a stainless steel autoclave. Afterwards, the screws of the autoclave were made tight to avoid the detonation of solution at the time of hydrothermal reaction. Then the autoclave was kept in a programmable hot air oven. In the oven, the hydrothermal reaction was performed at  $160^\circ\text{C}/8$  h. After completion of reaction, the oven was cooled down to room temperature. In next step, the sample was removed from the Teflon-linked bowl and then cleaned for 10–12 times until the pH reaches 7. Later on, the powder sample was dried at  $60^\circ\text{C}$  for 2 h in the hot air oven. The dried  $\text{MgFe}_2\text{O}_4$  nanopowder was grinded in agate mortar for 15 min to achieve the homogeneous powder particles. Finally,  $\text{MgFe}_2\text{O}_4$  (MF) nanoparticle samples characterized by XRD, FE-SEM with EDX, UV-VIS, FT-IR, PL and VSM techniques for structural, morphology, optical, Photoluminescence, and magnetization properties of  $\text{MgFe}_2\text{O}_4$  nanoparticles.

## 3. RESULTS

### 3.1. STRUCTURAL PROPERTIES

The XRD pattern of  $\text{MgFe}_2\text{O}_4$  (MF) nanoparticles was synthesized via the hydrothermal method are shown in Fig.1. All the observed different peaks corresponding to planes (111), (220), (311), (400), (420), (511), (440), (620), (533), and (444) were confirmed pattern in cubic spinel structure JCPDS card No. 89-3084. The  $\text{MgFe}_2\text{O}_4$  crystallite size (D) is calculated using the Debye-Scherrer formula by sharp Bragg reflection corresponding to the highest intense peak (311) about 36.6 nm. The obtained data indicated that the lattice constants  $a = b = c$  were  $8.3712 \text{ \AA}$  and in the unit cell volume ( $V = a^3$  for spinel cubic unit cell) value is  $586.63 \text{ \AA}^3$ . Herein, we can understand the variation of lattice constant based on the Shannon ionic radii data [16], and probable cation distribution. Shannon ionic radii data showed the ionic radii of different cations of  $\text{MgFe}_2\text{O}_4$  such as  $\text{Mg}^{+2}$ :  $0.72 \text{ \AA}$ ,  $\text{Fe}^{+3}$ :  $0.039 \text{ \AA}$ , and  $\text{O}^{-2}$ :  $0.068 \text{ \AA}$ . The evaluation of x-ray density is done by using equation [\*\*]  $\rho_x = 8\text{MW}/\text{NV}$ , where MW is molecular weight, N is Avogadro number ( $6.023 \times 10^{23}$ ), and V is Unit cell volume of magnesium ferrite nanoparticles for calculate the x-ray density value is  $4.531 \text{ g/cm}^3$ . Finally, the surface area (S) for all the samples was found using the formula:  $S = 6000/(D \cdot \rho_x)$ , where the symbols have their usual meaning. The 'S' was  $36.184 \text{ m}^2/\text{g}$  for  $\text{MgFe}_2\text{O}_4$  nanoparticles [17]. The  $\text{MgFe}_2\text{O}_4$  nanoparticles were determined dislocation density ( $\rho$ ), Atomic Packing Factor and Specific Surface area to volume ratio were obtained values listed in the Table.1.

Table.1. Data on the XRD structural and physical parameters of  $\text{MgFe}_2\text{O}_4$  nanoparticles

Data on XRD analysis of MF nanoparticles		
1.	Lattice parameter ( $a=b=c$ )	$8.3712 \text{ \AA}$
2.	MW	$199.993 \text{ g/mol}$
3.	Crystallite Size (D)	$36.6 \text{ nm}$
4.	Atomic Packing Factor	$0.1243$
5.	Volume (V)	$586.63 (\text{ \AA}^3)$
6.	Dislocation density ( $\rho$ )	$7.465\text{E}+14$
7.	X-Ray density ( $\rho_x$ )	$4.531 \text{ g/cm}^3$
8.	Surface Area (S)	$36.184 \text{ m}^2/\text{g}$
9.	S/V	$0.0617$

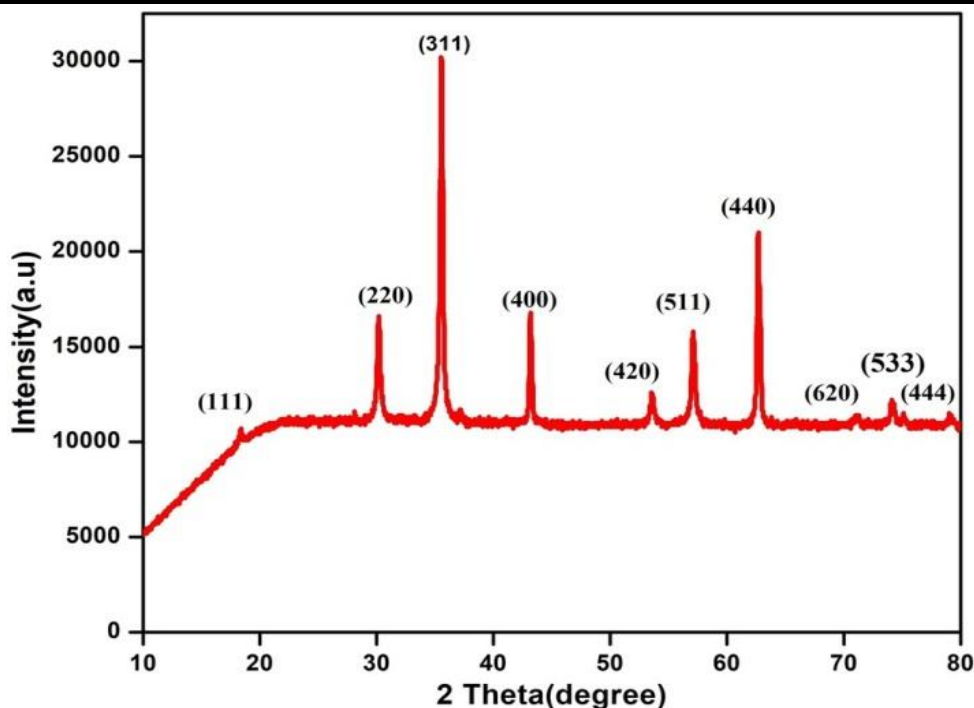


Fig.1. XRD pattern of MgFe<sub>2</sub>O<sub>4</sub> nanoparticles

### 3.2.OPTICAL PROPERTIES

Using the diffuse reflectance spectra (inset of Fig.2) of MgFe<sub>2</sub>O<sub>4</sub> nanoparticles, the optical band-gap ( $E_g$ ) was found for MgFe<sub>2</sub>O<sub>4</sub> nanoparticles. For this, the  $(\alpha h\nu)^n$  versus  $h\nu$  plots (where ' $\alpha$ ' is absorptivity, and ' $h\nu$ ' is the photon energy) were tense by consider  $n = 2$ . Since,  $n = 2$  is allowed for direct transition of charge carriers between the two energy bands [16]. We noticed from  $(\alpha h\nu)^2$  versus  $h\nu$  plots that the  $E_g$  value was 1.09 eV for MgFe<sub>2</sub>O<sub>4</sub> nanoparticles. The  $E_g$  value was determined by extrapolating the linear portion of the plots (Fig.2) towards the photon energy axis wherein, exactly, the absorptivity identical to zero [16]. In reference [19], it was found that for different Zn-contents ranging from 0.1 – 0.9, the  $E_g$  was varied from 0.935 – 1.524 eV. However, in this work, the numerical value of  $E_g$  was  $\sim 1.1$  eV due to the presence of MgFe<sub>2</sub>O<sub>4</sub> nanoparticles. Therefore, these wide band gap compositions can be expected for optoelectronic and sensor device applications [17, 18].

FT-IR spectra of MgFe<sub>2</sub>O<sub>4</sub> nanoparticles at room temperature are shown in Fig.3. Two major absorption bands were observed in the range of 430-580 cm<sup>-1</sup> confirming the formation of spinel ferrites; a high frequency band ( $\nu_a = 580$  cm<sup>-1</sup>) caused by the stretching vibrations of the tetrahedral metal –oxygen bond a low frequency ( $\nu_b = 430$  cm<sup>-1</sup>) due to the metal – oxygen vibrations in octahedral sites. [20].

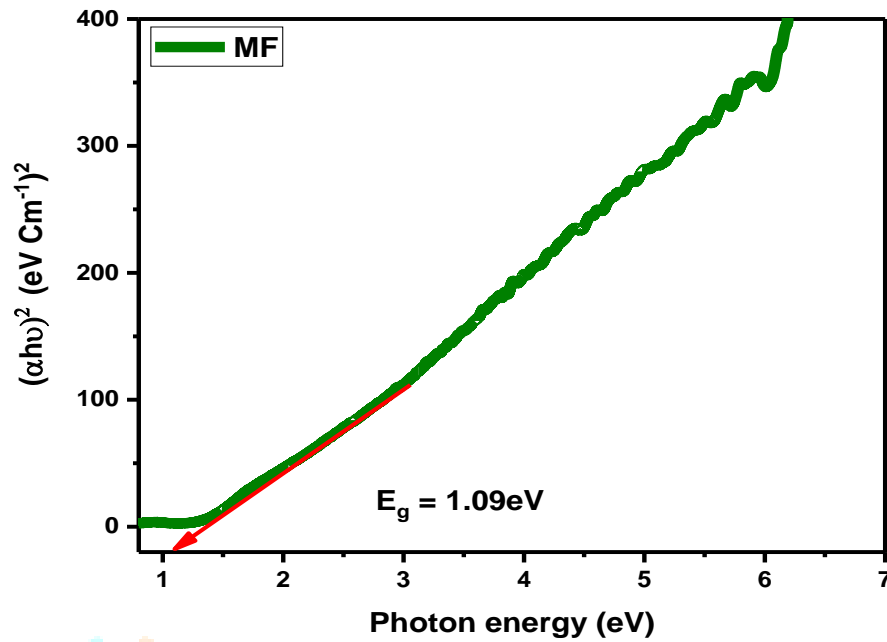


Fig.2. Optical band gap determination of MgFe<sub>2</sub>O<sub>4</sub> nanoparticles

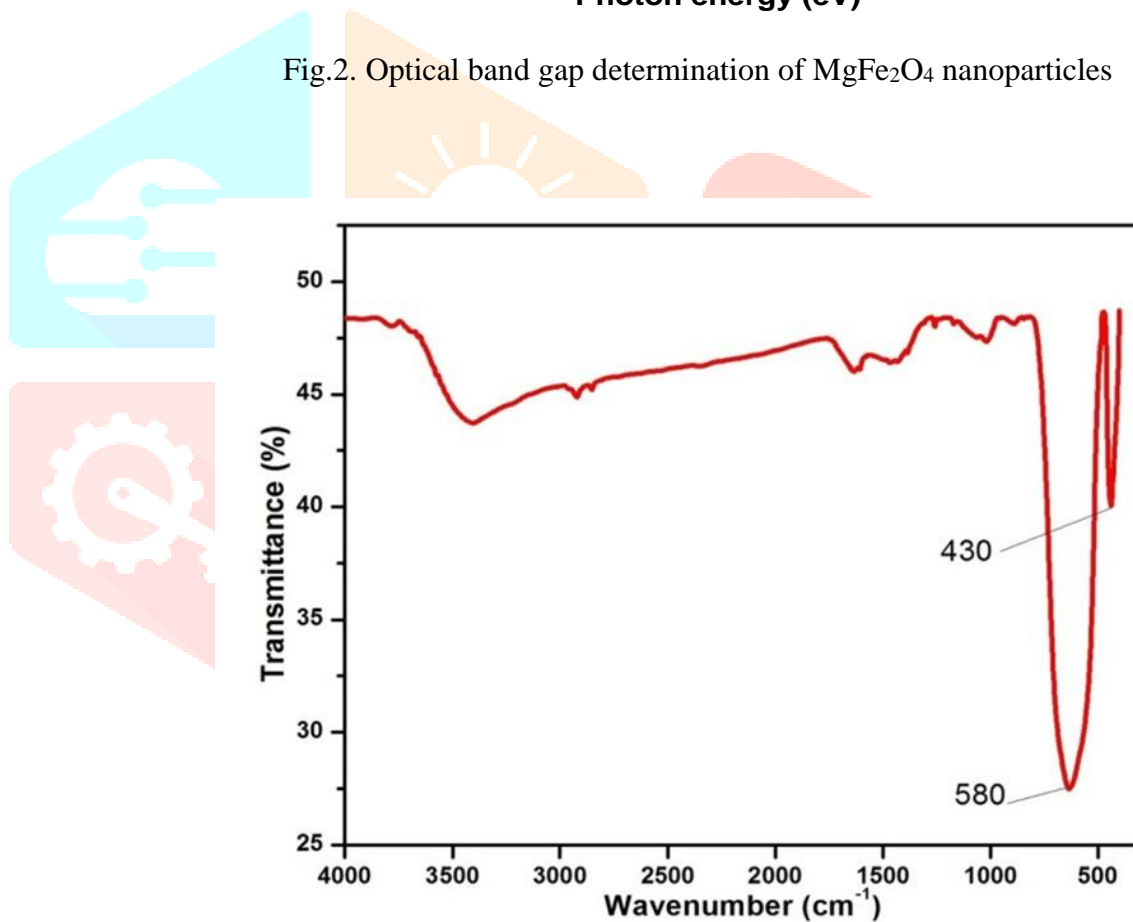


Fig.3. FT-IR Spectra of MgFe<sub>2</sub>O<sub>4</sub> nanoparticles

The Fig.4 shows PL spectra of MgFe<sub>2</sub>O<sub>4</sub> nanoparticles at room temperature. The emission peaks were noticed in the visible range of 380 nm to 560 nm, having a maximum near 425 nm. The MgFe<sub>2</sub>O<sub>4</sub> nanoparticles exhibited intense and broad blue emission between 380 nm to 499 nm with peak PL intensity at 425 nm. The emission between 499 nm to 560 nm is related to a weak green emission. Such electronic emission may be due to the radioactive defects at grain boundaries [20, 21] and the oxygen vacancies within the crystal structure [22].

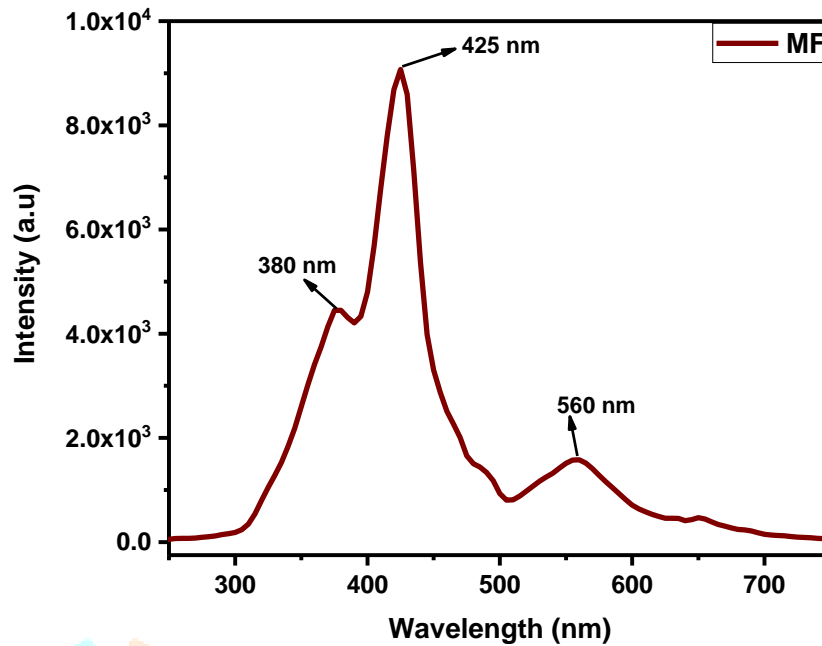


Fig.4. PL Spectra of  $\text{MgFe}_2\text{O}_4$  nanoparticles

### 3.3. MORPHOLOGICAL PROPERTIES

Field Emission scanning electron microscopy (FE-SEM) was carried on the way to observe morphology of the synthesized product. Fig. 5 shows the observed FE-SEM images clearly revealed that the magnetic ferrite particles are formed with some agglomeration at nanoscale. The particles have homogenous distribution. Agglomeration was also observed as small particles aggregated in order to achieve lower free energy state. Fig.6 shows the energy dispersive spectrum (EDS) for  $\text{MgFe}_2\text{O}_4$  nanopowder and Table 2 gives quantitative estimation of elements obtained directly from spectrum through its atomic and weight percentages values. The results were confirmed the presence of required elements in the prepared composition with almost all the peaks associated with elements such as those of Mg, Fe, O, thereby suggesting the formation of  $\text{MgFe}_2\text{O}_4$  nanoparticles [18].

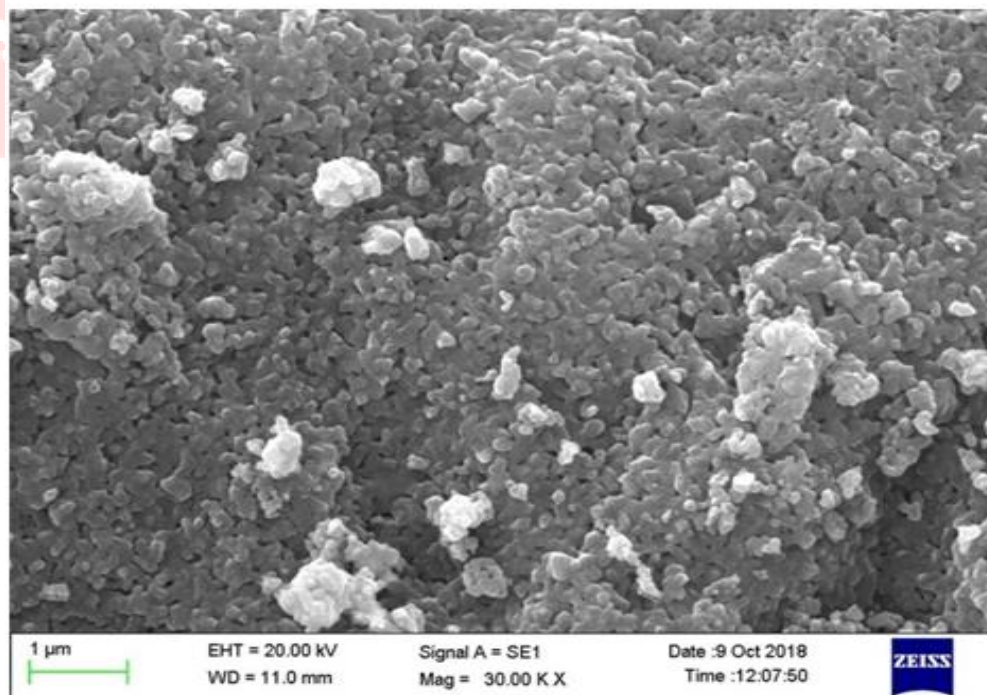
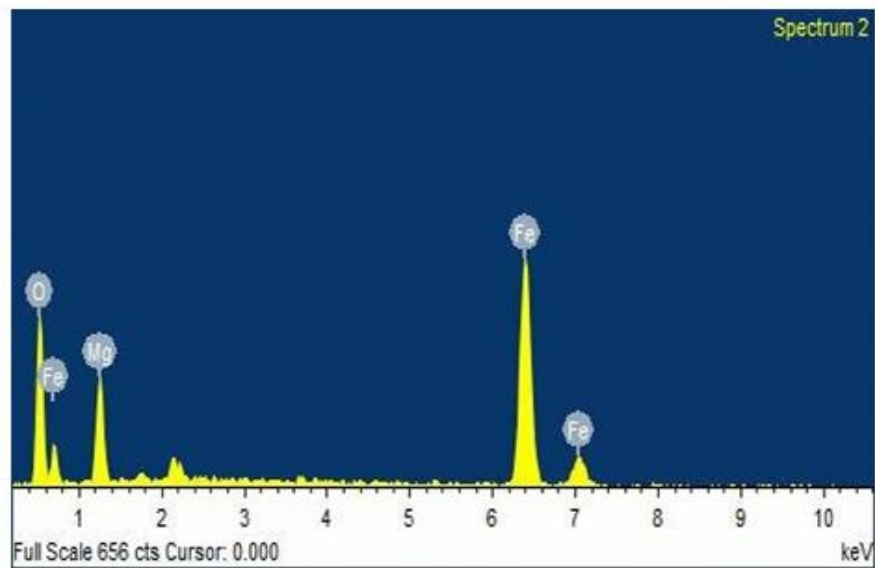


Fig.4. FE-SEM image of  $\text{MgFe}_2\text{O}_4$  nanoparticles



Fig.5. EDX of MgFe<sub>2</sub>O<sub>4</sub> nanoparticlesTable.2. Atomic Percentage of MgFe<sub>2</sub>O<sub>4</sub> nanoparticles

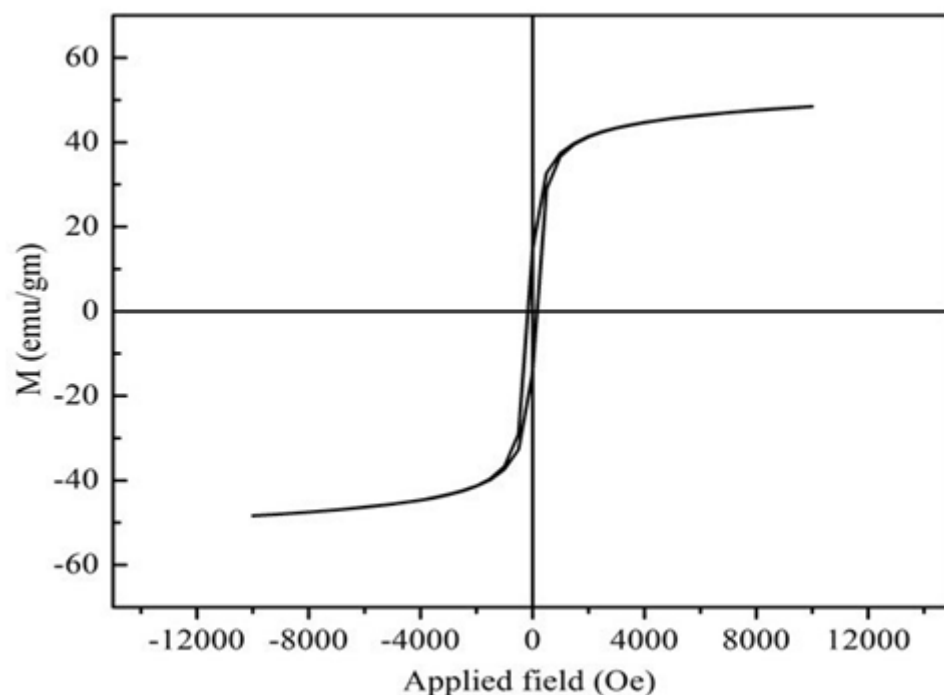
Composition	Atomic percentage (At %)		
	Mg	Fe	O
Mg Fe <sub>2</sub> O <sub>4</sub>	15.96	31.46	52.58

### 3.4. MAGNETIC PROPERTIES

The hysteresis or loop is used to determine the behavior of ferromagnetic materials when placed in the magnetic field. Fig.7 displays the room temperature hysteresis loop for MgFe<sub>2</sub>O<sub>4</sub> nanoparticles are prepared by hydrothermal method, which indicates the soft magnetic nature of the synthesized particles. The values of the saturation magnetization ( $M_s$ ), coercivity ( $H_c$ ), retainivity ( $M_R$ ) and  $M_R/M_s$  ratio were obtained from this curve as 48.40 emu/g, 169.25 Oe, 14.47 emu/g and 0.2989 respectively as shown in Table.3. [23].

Table.3. Data on the Magnetic parameters of MgFe<sub>2</sub>O<sub>4</sub> nanoparticles

Compositio n	$M_s$ (emu/g)	$M_R$ (emu/g)	$H_c$ (Oe)	$M_R/M_s$ ratio
MgFe <sub>2</sub> O <sub>4</sub>	48.4	14.47	169.25	0.2989

Fig.5.M-H loop of MgFe<sub>2</sub>O<sub>4</sub> nanoparticles

## CONCLUSION

Hydrothermal method in compare to further synthesis methods of nanoparticles preparation has many advantages, for examples: easy, accessible, and low-cost. In this work, we have prepared the  $MgFe_2O_4$  nanoparticles synthesized through hydrothermal method. X-ray analysis confirmed the formation of a cubic spinel structure. FTIR result confirmed the ferrite phase formation. FE-SEM images illustrate that the magnetic ferrite particles are formed with various agglomeration at nanoscale. The EDX results confirm the presence of the required elements in the prepared composition. The optical energy band gap of 1.09 eV, preserve is providing the applications in sensor and optoelectronic devices. The room temperature M-H loop of the sample tends to be ferromagnetic in nature. The values of the saturation magnetization ( $M_S$ ), coercivity ( $H_C$ ), retativity ( $M_R$ ) and  $M_R / M_S$  ratio were obtained from this curve as 48.40 emu/g, 169.25 Oe, 14.47emu/g and 0.2989 respectively.

## ACKNOWLEDGEMENTS

The authors expressed thankfulness to Dr. M. V. Lakshmaiah, Professor (Physics & Electronics), Department of Physics, Sri Krishnadevaraya University, Ananthapuramu, for providing Research Lab, My special thanks go to SRMIST consultancy, SRM University, Chennai for providing me the necessary characterizations ( FTIR, and UV-Vis), XRD and PL & FE-SEM with EDX providing Yogi Vemana University, YSR Kadapa and IISc, Bangalore, respectively.

## REFERENCES

1. Peredkov, S.; Neeb, M.; Eberhardt, W.; Meyer, J.D.; Tombers, M.; Kampschulte, H.; Niedner-Schatteburg, G. Spin and orbital magnetic moments of free nanoparticles. *Phys. Rev. Lett.* 107 (2011) 233401.
2. Salunkhe, A.; Khot, V.M.; Phadatare, M.R.; Pawar, S.H. Combustion synthesis of cobalt ferrite nanoparticles—Influence of fuel to oxidizer ratio. *J. Alloys Compd.* 514 (2012) 91–96.
3. Kefeni, K.K.; Msagati, T.A.; Mamba, B.B. Ferrite nanoparticles: Synthesis, characterisation and applications in electronic device. *Mater. Sci. Eng. B* 215 (2017) 37–55.
4. J Emima Jeronsia, L Allwin Joseph, M Mary Jaculin, P Annie Vinosha, S Jerome Das, Hydrothermal synthesis of zinc stannate nanoparticles for antibacterial applications, *JTUSCI* Doi:10.1016/j.jtusci.2015.12.003.
5. Maaz, K.; Mumtaza, A.; Hasanaina, S.K.; Ceylan, A. Synthesis and magnetic properties of cobalt ferrite ( $CoFe_2O_4$ ) nanoparticles prepared by wet chemical route. *J. Magn. Mater.* 308 (2007) 289–295.
6. Shudan Li, Xianlei Wang, Synthesis of different morphologies lanthanum ferrite ( $LaFeO_3$ ) fibers via electrospinning, *Optik*, 126 (2015) 408-410.
7. AB Salunkhe, VM Khot, MR Phadatare, SH Pawar, Combustion synthesis of cobalt ferrite nanoparticles - Influence of fuel to oxidizer ratio, *J. Alloys comp*, 514 (2012) 91-96.
8. AK Nikumbh, , RA Pawar, DV Nighot, GS Gugale, MD Sangale, MB Khanvilkar, AV Nagawade, Structural, electrical, magnetic and dielectric properties of rare-earth substituted cobalt ferrites nanoparticles synthesized by the co-precipitation method, *J. Magu. Magn. Mater.*, 355 (2014) 201-209.
9. Huma Malik, Azhar Mahmood, Khalid Mahmood, Maria Yousaf Lodhi, Muhammad Farooq Warsi, Imran Shakir, Hassan Wahab, M. Asghar, Muhammad Azhar Khan, Influence of cobalt substitution on the magnetic properties of zinc nanocrystals synthesized via micro-emulsion route, *Ceram. Int.*, 40, (2014), 9439-9444.
10. Yarilyn Cedeno-Mattei, Oscar Perales-Perez, Oswald N.C. Uwakweh, Effect of high- energy ball milling time on structural and magnetic properties of nanocrystalline cobalt ferrite powders, *J. Magu. Magn. Mater.*, 341 (2013) 17-24.
11. Tal Meron, Yuri Rosenberg, Yossi Lereah, Gil Markovich, Synthesis and assembly of high-quality cobalt ferrite nanocrystals prepared by a modified sol-gel technique, *J. Magu. Magn. Mater.*, 292 (2005) 11-16.
12. Ningzhong B, Liming S, Yuhsiang W, Prahallad P, Arunava G, A facile thermolysis route to monodisperse ferrite nanocrystals. *J Am Chem* 129(41), (2007) 12374–12375
13. Iqbal T, Hassan A, Ghazal S, Wet chemical co-precipitation synthesis of nickel ferrite nanoparticles and their characterization. *J Inorg Organomet Poly Mater* 27 (2017) 1430–1438.

14. Bennet J, Tholkappiyan R, Vishista K, Victor JN, Hamed F, Attestation in self-propagating combustion approach of spinel  $AFe_2O_4$  ( $A = Co, Mg$  and  $Mn$ ) complexes bearing mixed oxidation states: Magnetostructural properties. *Appl Surf Sci* 383: (2016) 113–125.
15. Rashad MM, Soltan S, Ramadan AA, Bekheet MF, Rayan DA, Investigation of the structural, optical and magnetic properties of  $CuO/CuFe_2O_4$  nanocomposites synthesized via simple microemulsion method. *Cer Int* 41(9): (2015) 12237–12245.
16. R.D. Shannon, Revised effective ionic radii and systematic studies of interatomic distances in halides and chalcogenides. *Acta Cryst. A* 32, (1976) 751–767.
17. N. Raghuram, T.S. Rao, K. Chandra Babu Naidu, Investigations on functional properties of hydrothermally synthesized  $Ba_{1-x}Sr_xFe_{12}O_{19}$  ( $x = 0.0-0.8$ ) nanoparticles. *Mater. Sci. Semicond. Process.* 94, (2019) 136–150.
18. D.Chinna Venkata Subbaiah, S Dastagiri, G.Pakardin, G. Md. Dastageer, M.V. Lakshmaiah, Synthesis And Investigation of Cobalt Ferrite Nanoparticles: Structural, Morphological, Optical, Magnetic, and Dielectric Properties, *International Journal of Engineering Research & Technology*, Vol. 12 Issue 01, (2023) 13-21.
19. Y.Abubakar, A.Zulkifly, A.I.Nor, Hashim Mansor, Effect of temperature on structural, magnetic and dielectric properties of cobalt ferrite nanoparticles prepared via co-precipitation method, *Phys.Sci. Inter. J.* 8 (1) (2015) 1-8.
20. C. H. Zang, D. M. Zhang, C.J. Tang, S.J. Fang, Z.J. Zong, Y.X. Yang, C. H. Zhao, Y. S. Zhang, Optical properties of a  $ZnO/P$  nanostructure fabricated by a chemical vapor deposition method, *J. Phys. Chem. C* 113 (2009), 18527.
21. L.J. Zhuge, X. M Wu., X. M Yang, Q. Chen, Structural and deep ultraviolet emission of Co-doping  $ZnO$  films with  $Co_3O_4$  nano-clusters, *J. Mater. Chem. Phys.* 120 (2010) 480 – 483.
22. R. Bhargava, P. K. Sharma, R. K. Dutta, S. Kumar, A.C. Pandey, N. Kumar, Influence of Co-doping on the thermal, structural, and optical properties of sol-gel derived  $ZnO$  nanoparticles, *J. Mater. Chem. Phys.* 120 (2010) 393.
23. Harshal B. Desai, Arun Kumar and Ashish R. Tanna, Structural and Magnetic properties of  $MgFe_2O_4$  ferrite nanoparticles synthesis through auto combustion technique, *Eur. Chem. Bull.* 10(3), (2021) 186-190.

